GRID-CONNECTED PHOTOVOLTAIC SYSTEMS WITH DUAL INVERTERS WITH SYNCHRONIZED SPACE-VECTOR MODULATION

OLESCHUK Valentin, SIZOV Alexandr
Power Engineering Institute of the Academy of Sciences of Moldova

Abstract – *Photovoltaic (PV) systems, controlled by the means of modern power electronics, are now important renewable power sources of the energy complex. One of perspective topologies of PV systems is based on two insulated strings of PV panels, feeding two voltage source inverters. These two i**nverters are connected to the grid by a three-phase transformer having open-end windings on inverters side**. Strategy of control and modulation of dual inverters, based on a**lgorithms of synchronized modulation,** has been presented, allows providing continuous phase voltage synchronization for any operation condition of photovoltaic systems.*
Keywords – *photovoltaic string, voltage source inverter, synchronized space-vector modulation*

SISTEME FOTOVOLTAICE ÎN BAZA INVERTOARELOR DUBLE CU MODULAREA SINCRONĂ VECTORIALĂ RACORDATE LA REŢEA

OLESCIUK Valentin, SIZOV Alexandr
Institutul de Energetică al Academiei de Ştiinţe a Moldovei

Rezumat – *Sisteme fotovoltaice bazate pe instalaţii electronice de putere moderne, reprezintă surse importante de energie regenerabilă. Una dintre cele mai de perspectivă topologii a acestor sisteme include în componenţa sa două module de bază, compuse din celule fotovoltaice şi conectate la intrările celor două invertoare de tensiune. Invertoarele menţionate sunt racordate la reţea printr-un transformator trifazat cu înfăşurări decuplate din partea invertorului. Se descrie şi se analizează strategia de dirijare a invertoarelor dublate în baza algoritmilor modulării prin impulsuri de durată variabile de tip sincron, asigurând simetria curbelor tensiunii de ieşire în diferite condiţii de funcţionare a sistemei fotovoltaice.*
Cuvinte cheie – *module fotovoltaice, invertorul de tensiune, modularea vectoriala de tic sincron*

СВЯЗАННЫЕ С СЕТЬЮ ФОТОПРЕОБРАЗОВАТЕЛЬНЫЕ СИСТЕМЫ НА БАЗЕ СДВОЕННЫХ ИНВЕРТОРОВ С СИНХРОННОЙ ВЕКТОРНОЙ МОДУЛЯЦИЕЙ

Олещук В., Сизов А.
Институт энергетики Академии наук Молдовы

Реферат – *Фотопреобразовательные системы на базе современных устройств силовой электроники являются в настоящее время важными источниками возобновляемой энергии. Одна из перспективных топологий таких систем включает в свой состав два базовых модуля, составленных из фотопреобразовательных ячеек ,и соединенных со входами двух инверторов напряжения. Указанные инверторы подключены к сети через трехфазный трансформатор с разомкнутыми обмотками на инверторной стороне. Описывается и анализируется стратегия регулирования сдвоенных инверторов на базе алгоритмов синхронной широтно-импульсной модуляции, обеспечивающих симметрию кривых фазного выходного напряжения при различных условиях функционирования фотопреобразовательной системы.*
Ключевые слова *– фотопреобразовательная панель, инвертор напряжения, синхронная векторная модуляция*

1. INTRODUCTION

Photovoltaic (PV) based power systems are one of the most promising installations between modern renewable energy systems. [1]-[6]. Power electronic converters are basic components of PV systems. Every year the price pr. produced kWh is decreasing by improving the PV-cells themselves as well as making the PV-inverters more efficient and cheaper. The annual installation of PV power has increased to above 7 GWp leading to cumulative installed PV power by the end of 2009 reaching to approximately 15 GWp, which actually is about 10 % of the wind power capacity. Fig. 1 shows the cumulative PV installed capacity [5].

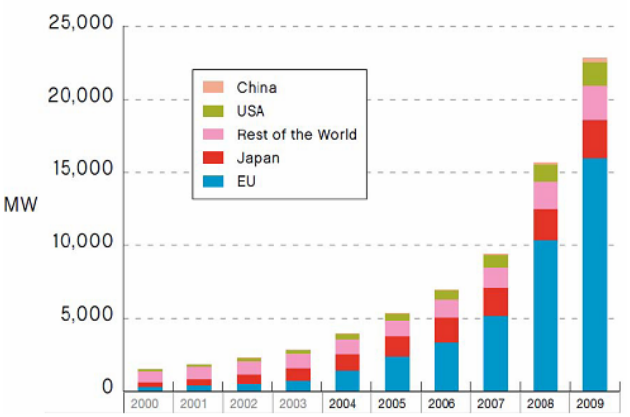

Fig. 1. Cumulative PV installed capacity from 2000 to 2009 [5]

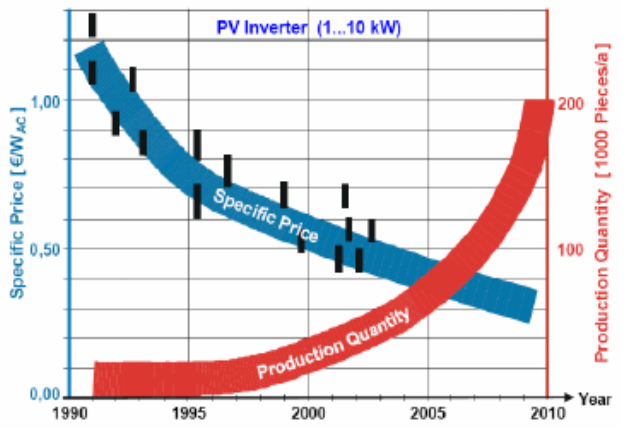

Fig. 2. Development and prognosis of specific cost and production quantity for the PV inverter of nominal powers between 1 and 10 kW during two decades [5]

The vast majority of new capacity during the last years was installed in EU with Germany as dominating the market followed by Spain and Italy. USA market is growing fast especially after the new incentive policy in California while Japan now is growing slowly after being a leading country [5].

2. PRICE DECREASING TENDENCY

According to prognoses, the prices for PV modules are decreased by the end of 2012 to less than 1.5 €/Wp with stronger trends for using thin film technology in order to reach the psychological threshold of 1 €/Wp, which really will trigger the mass-penetration of PV as an energy and power source [4].

In addition to the PV module cost, the cost and reliability of PV inverters are also important issues. The inverter cost share represents about 10-15% of the total investment cost of a grid connected PV system [5].

The prices for PV inverters in the 1-10 kW range are shown in Fig. 2. It can be seen that the inverter cost of this power class has decreased by more than 50 % during the last decade. The main reasons for this reduction are the increase of the production quantities and the implementation of new system technologies (e.g. string-inverters). A further 50% reduction of the specific cost is anticipated during the coming decade. The corresponding specific cost is expected to achieve below 0.3 €/WAC at the nearest years, which requires the implementation of specific measures in the development and the manufacturing processes [5].

3. GRID-CONNECTED PHOTOVOLTAIC SYSTEMS

Historically the main market segments for PV were the remote industrial and developing country applications where PV power over long term is often more costeffective than alternative power options such as diesel generator or mains grid extension [5]. Since 1997, the proportion of new grid-connected PV installed in the reporting countries rose from 42% to more than 93% in 2004 (see Fig. 3 and Fig. 4, [4]).

Worldwide, the cumulative share of off-grid to grid-connected applications is approximately 1:4 at the present time [6]. So, clear tendency of growing of total power of the grid-connected PV systems should be marked. However, this is not the case in every reporting country. In Sweden, Norway and Finland, the most common applications are for vacation cottages, while in Australia, Mexico, and France achieving rural electrification is a key objective. In Canada, Israel and Korea, commercial and telecommunications applications dominate [5].

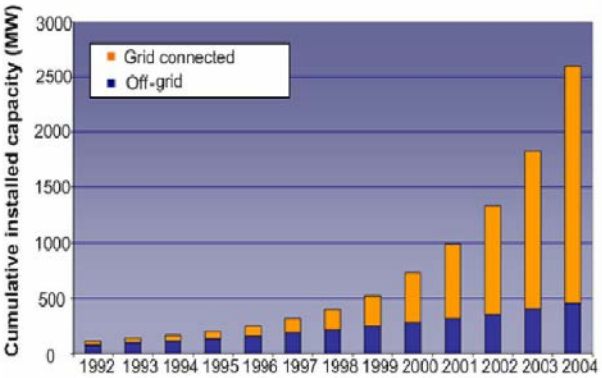

Fig. 3. Cumulative installed PV capacity from 1992 to 2004 [4]

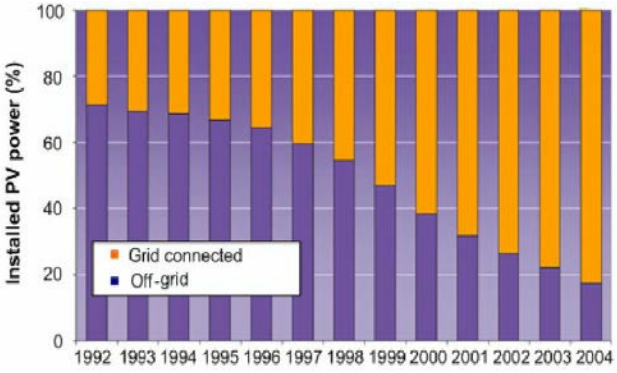

Fig. 4. Percentages of grid connected and off-grid PV power of installed PV capacity from 1992 to 2004 [4]

4. PHOTOVOLTAIC SYSTEM ON THE BASE OF DUAL INVERTERS WITH SYNCHRONIZED PWM

Novel topology of grid-connected photovoltaic systems has been recently proposed ([7],[8]). This structure is based on two PV modules, each one feeding the dc bus of three-phase voltage source inverter. Two inverters are connected to the grid by a three-phase transformer having open-end windings on inverters side.

Fig. 5 presents photovoltaic system based on dual neutral-point-clamped inverters supplied by two insulated strings of photovoltaic panels with the resulting dc voltages V_{dc1} and V_{dc2}. Direct connection of photovoltaic modules to inverters, or their connection through dc/dc link (dashed blocks in Fig. 5) is available in this case. Dual neutral-point-clamped inverters are connected to grid by a three-phase transformer with the open winding configuration on primary side, and this configuration is one of the most suitable for photovoltaic systems with an increased power range [9].

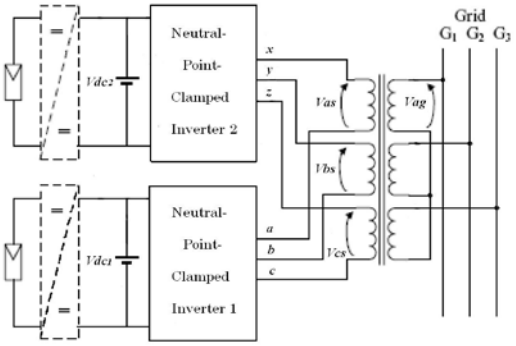

Fig. 5. Topology of photovoltaic system on the base of dual neutral-point-clamped inverters [9]

4.1 Three-phase neutral-point-clamped inverter

Fig. 6 presents basic topology of neutral-point-clamped inverter (of the first inverter with the phases ***a, b, c***). Each of three legs of the inverter consists of four power switches, four freewheeling diodes and two clamping diodes. Fig. 7 shows the switching state vectors of the inverter. Generally, there are twenty-seven different switching states, which correspond to nineteen vectors shown by the big and small arrows in Fig. 10 [9]. Recently, new schemes of pulsewidth modulation have been proposed for three-level inverters, providing elimination of undesirable alternating common-mode voltages in adjustable speed drive systems and other applications [10]-[11]. So, it is leading to an increase of the reliability of power conversion systems.

Twelve (six and six) switching state vectors are located on the periphery of the two presented hexagons, and six small vectors have the position in the middle of the corresponding big vectors. There is also a zero voltage vector. Generally, it can be represented by three different switching states. It is known, that the use of only seven of the vectors, $\boldsymbol{V_1}$ - $\boldsymbol{V_7}$, marked in Fig. 7 by the big arrows with the corresponding number of vector, can provide elimination of the common-mode voltages in a three-

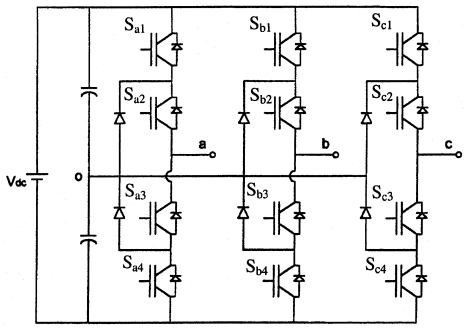

Fig. 6. Topology of three-phase neutral-point-clamped inverter

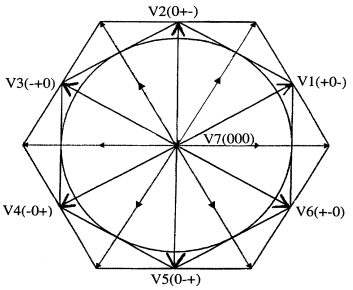

Fig. 7. Switching state vectors providing elimination of the common-mode voltages in the load

phase load [9]-[11]. A ternary switching variable (**+**,**0**,**-**) is defined for the switches of each of the three phase as:

+ *if* $\boldsymbol{S_1}$, $\boldsymbol{S_2}$ *are* ***ON*** *and* $\boldsymbol{S_3}$, $\boldsymbol{S_4}$ *are* ***OFF***;

0 *if* $\boldsymbol{S_2}$, $\boldsymbol{S_3}$ *are* ***ON*** *and* $\boldsymbol{S_1}$, $\boldsymbol{S_4}$ *are* ***OFF***;

- *if* $\boldsymbol{S_3}$, $\boldsymbol{S_4}$ *are* ***ON*** *and* $\boldsymbol{S_1}$, $\boldsymbol{S_2}$ *are* ***OFF***.

Switching state sequences can be written in this case for the corresponding vectors as:

$$\boldsymbol{V_1\,(+0-);\ V_2\,(0+-);\ V_3\,(-+0);\ V_4\,(-0+);}$$

$$\boldsymbol{V_5\,(0-+);\ V_6\,(+-0);\ V_7\,(000)}.$$

4.2 General scheme of continuous synchronization of output voltage waveforms of three-phase inverters

In order to avoid asynchronism of conventional schemes of voltage space-vector modulation, a novel method of synchronized PWM can be used for control of three-phase neutral-point-clamped inverters [12]. Fig. 8 presents (for the first 60^0-clock-interval) switching state sequence, the pole voltages V_a and V_b, and the line-to-line voltage V_{ab} of neutral-point-clamped inverter with continuous scheme of synchronized PWM, providing both alternating common-mode voltage elimination and continuous voltage synchronization in the system [12].

In particular, in Fig. 8 the signals βj represent the total active switching state durations during the switching period (sub-cycle) τ, and the signals γ_k are generated on the boundaries of the corresponding β–signals. Widths of notches λ_j represent zero sequences.

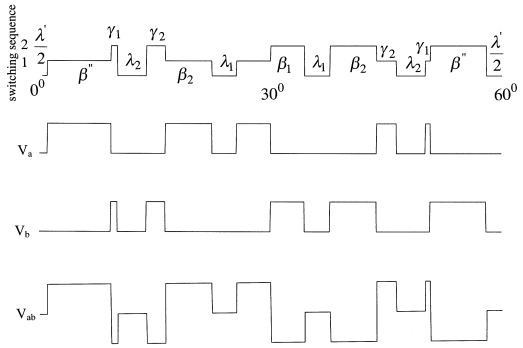

Fig. 8. Switching state sequence, pole voltages V_a, V_b, and line voltage V_{ab} of converter with continuous synchronized PWM for the first 60^0-clock-interval

So, one of the basic ideas of the proposed PWM method is in continuous synchronization of positions of all central signals β_1 in the centres of the 60^0-clock-intervals (to fix positions of the β_1-signals in the centres of the 60^0-cycles), and in symmetrical generation of all other active β- and γ-signals, together with the corresponding notches, around of these central signals.

Determination of duration of sub-cycles τ as a function of switching frequency F_s is based on (1) for the continuous (CPWM [9],[11],[12]) and "direct-direct" (DDPWM, [10],[13]) schemes of synchronized PWM, and on (2) for the discontinuous (DPWM [9],[13]) scheme of PWM:

$$\tau_{CPWM,DDPWM} = 1/2F_s \tag{1}$$

$$\tau_{DPWM} = 1/1.5F_s \tag{2}$$

Equations (3)-(8) present a set of control functions for determination of duration of signals of neutral-point-clamped inverters with synchronized PWM in absolute values (seconds) [9],[12]:

For *j=2,...i-1:*

$$\beta_j = \beta_1 \cos[(j-1-K_1)\tau] \tag{3}$$

$$\gamma_j = \beta_{i-j+1}\{0.5 - 0.87\tan[(i-j-K_1)\tau]\} \tag{4}$$

$$\beta_i = \beta'' = \beta_1 \cos[(i-K_1-1)\tau]K_s \tag{5}$$

$$\gamma_1 = \beta''\{0.5 - 0.87\tan[(i-K_1-2)\tau + (\beta_{i-1}+\beta_i+\lambda_{i-1})/2]\}K_s \tag{6}$$

$$\lambda_j = \tau - (\beta_j + \beta_{j+1})/2 \tag{7}$$

$$\lambda_i = \lambda' = \left(\tau - \beta''\right)K_s, \tag{8}$$

where: $m=V/V_{max}$ – modulation index of each inverter, $\beta_1 = 1.1\tau m$, K_s – coefficient of synchronization [12], $K_1=0$ (for continuous and "direct-direct" PWM), and $K_1=0.25$ (for discontinuous synchronized pulsewidth modulation).

4.3 Operation of dual-inverter system with algorithms of synchronized PWM

Synchronous control of the output voltage of each inverter of dual-inverter system with synchronized PWM provides synchronous symmetrical regulation of the phase voltages V_{as}, V_{bs} and V_{cs} of the system (Fig. 5). Rational phase shift between output voltage waveforms of the two neutral-point-clamped inverters is equal in this case to one half of the switching interval τ [13].

Taking into consideration the fact, that the analyzed control scheme provides full elimination of the common-mode voltages in the system, the phase voltages V_{as}, V_{bs} and V_{cs} of the dual-inverter system with two insulated dc-sources (Fig. 5) are calculated in accordance with (9)-(11) [14]:

$$V_{as} = V_a + V_x, \tag{9}$$

$$V_{bs} = V_b + V_y, \tag{10}$$

$$V_{cs} = V_c + V_z, \tag{11}$$

where V_a, V_b, V_c, V_x, V_y, V_z are the corresponding pole voltages of the two neutral-clamped inverters (Figs. 5-6).

In order to provide maximum power point tracking of photovoltaic panels during solar irradiance fluctuations, the corresponding control system has been elaborated and described for dual-inverter-based photovoltaic system [8].

As an example of operation of the system with dual neutral-point-clamped inverters with synchronized PWM with equal DC-voltages and currents, Fig. 9 – Fig. 14 present basic voltage waveforms (period of the pole voltages V_a, V_x,, line-to-line voltage V_{ab} of the two neutral-point-clamped inverters, and of the common-mode voltage V_0 and phase voltage V_{as} (with its spectra in Figs. 10,12,14) for dual-inverter photovoltaic installation.

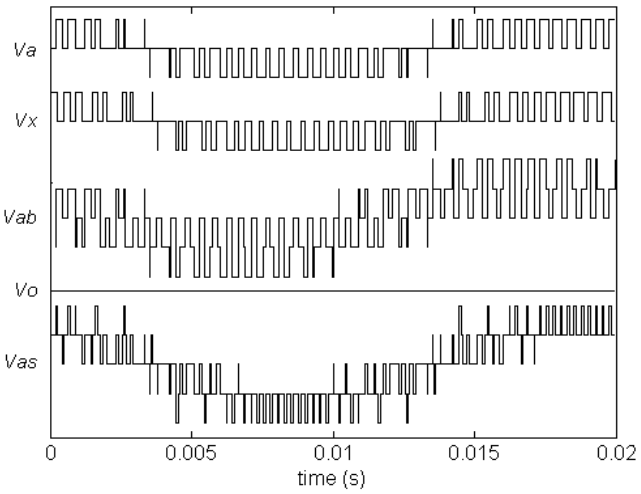

Fig. 9. Pole voltages V_a and V_x, line voltage V_{ab}, common-mode voltage V_0 and phase voltage V_{as} of the system with continuous synchronized PWM ($F=50Hz$, $F_s=1kHz$, $m_1=m_2=0.6$)

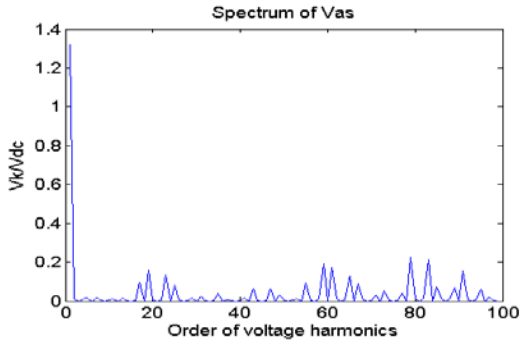

Fig. 10. Spectrum of the phase voltage V_{as} of the system with continuous synchronized PWM ($F=50Hz$, $F_s=1kHz$, $m_1=m_2=0.6$)

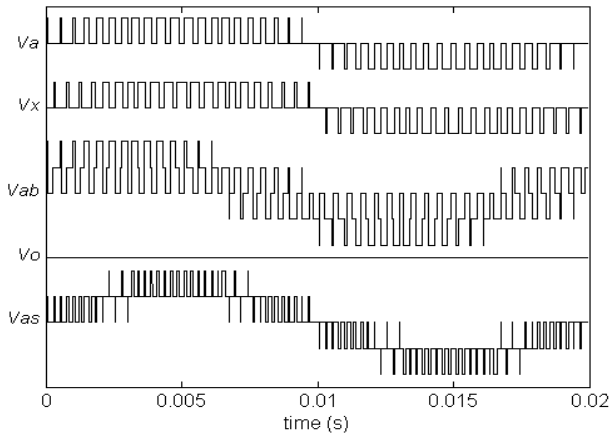

Fig. 11. Pole voltages V_a and V_x, line voltage V_{ab}, common-mode voltage V_0 and phase voltage V_{as} of the system with the "direct-direct" scheme of PWM ($F=50Hz$, $F_s=1kHz$, $m_1=m_2=0.6$)

The fundamental frequency of the system is $F = 50$ *Hz*, the average switching frequency is equal to $F_s = 1kHz$ for each inverter of the system, and modulation indices of the two inverters are $m_1=m_2=0.6$.

In particular, Fig. 9 shows basic voltage waveforms of the system controlled by algorithms of continuous synchronized PWM. Figs. 11-12 present voltage waveforms (with spectra of the V_{as} voltage) for the system with "direct-direct" PWM, which is one of the useful sub-versions of continuous PWM for neutral-point-clamped converters [9]-[10],[13]. Figs. 13-14 show voltage waveforms (with spectrum of the V_{as} voltage) for the system with discontinuous pulsewidth modulation.

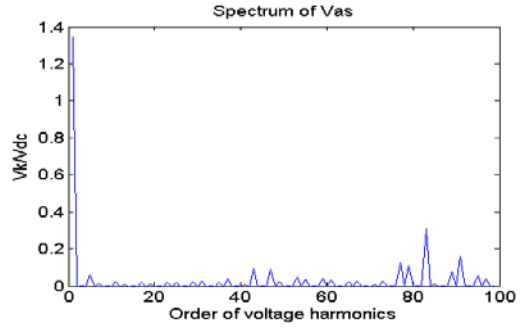

Fig. 12. Spectrum of the phase voltage V_{as} of the system with the "direct-direct" scheme of PWM ($F=50Hz$, $F_s=1kHz$, $m_1=m_2=0.6$)

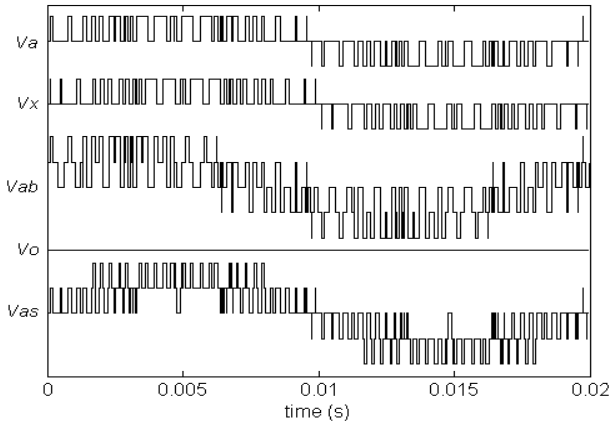

Fig. 13. Pole voltages V_a and V_x, line voltage V_{ab}, common-mode voltage V_0 and phase voltage V_{as} of the system with discontinuous synchronized PWM ($F=50Hz$, $F_s=1kHz$, $m_1=m_2=0.6$)

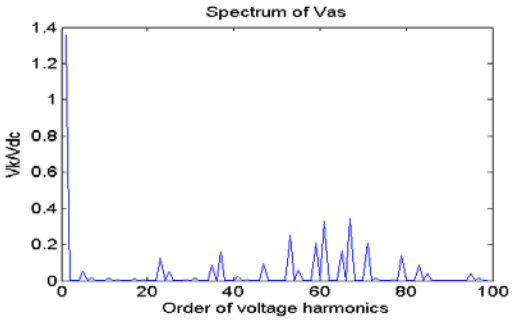

Fig. 14. Spectrum of the phase voltage V_{as} of the system with discontinuous synchronized PWM ($F=50Hz$, $F_s=1kHz$, $m_1=m_2=0.6$)

Analysis of spectral characteristics of the phase voltage of dual-inverter system shows (see Figs. 10, 12, 14), that spectra of the phase voltage of systems with synchronized PWM do not contain even harmonics and sub-harmonics for any control regime of photovoltaic systems.

4.4 Operation of photovoltaic system with non-equal currents of two dc-sources (photovoltaic strings)

In the case of different level of solar irradiance for the two strings of photovoltaic panels, the corresponding DC-currents of the system are different too. In order to provide maximum power point tracking of photovoltaic panels and stabilization of the magnitude of the fundamental harmonic of the phase current of a dual-inverter system, modulation indices m_1 and m_2 of the two inverters should be in direct proportional dependences with the corresponding DC-currents I_{dc1} and I_{dc2} [8].

Figs. 15-18 illustrate operation of the system with discontinuous PWM under condition $I_{dc2}=0.8I_{dc1}$ (Figs. 15-16, modulation indices are equal to $m_1=0.9$ and $m_2=0.72$ in this case), and under condition $I_{dc2}=0.6I_{dc1}$ (Figs. 17-18, $m_1=0.9$ and $m_2=0.54$ in this case). In particular, harmonic analysis of voltage waveforms shows (Figs. 16 and 18) that spectra of the phase voltage of dual-inverter systems with synchronized PWM do not contain

even harmonics and sub-harmonics in systems with non-equal currents of two dc-sources too.

Due to the specialized control scheme, based on the use of only seven voltage vectors, marked in Fig. 7, the alternative common-mode voltage V_0 is equal to zero for any operation conditions of the system with both equal (Figs. 9, 11, 13) and non-equal (Figs. 15, 17) dc-currents of two dc-sources. And the proposed PWM algorithms provide also close to constancy magnitude of the first (fundamental) harmonic of the phase voltage for any control mode of the system.

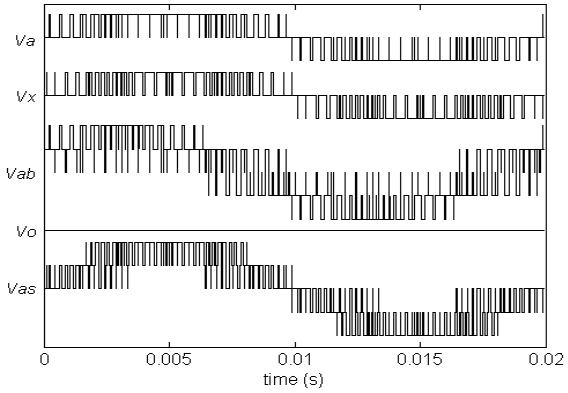

Fig. 15. Pole voltages V_a and V_x, line voltage V_{ab}, common-mode voltage V_0 and phase voltage V_{as} of the system with discontinuous synchronized PWM ($F=50Hz$, $F_s=1.5kHz$, $I_{dc1}=0.8I_{dc2}$, $m_1=0.9$, $m_2=0.72$)

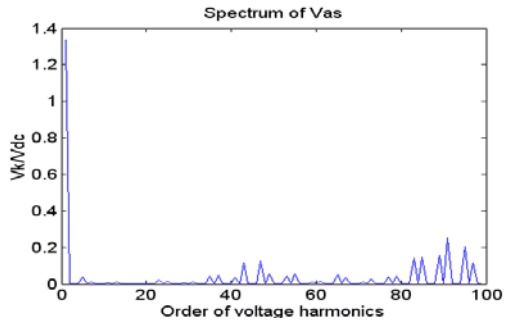

Fig. 16. Spectrum of the phase voltage V_{as} of the system

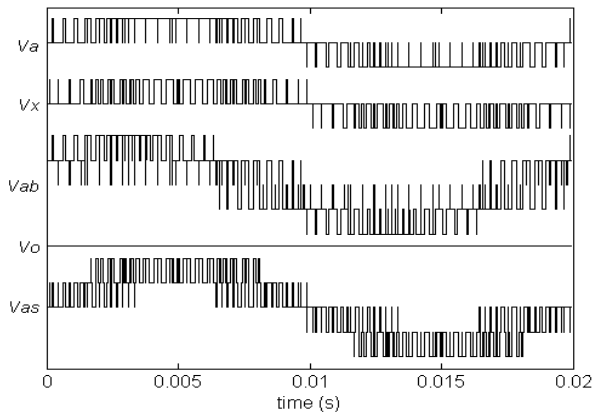

Fig. 17. Pole voltages V_a and V_x, line voltage V_{ab}, common-mode voltage V_0 and phase voltage V_{as} of the system with discontinuous synchronized PWM ($F=50Hz$, $F_{s2}=1.5kHz$, $I_{dc1}=0.6I_{dc2}$, $m_1=0.9$, $m_2=0.54$)

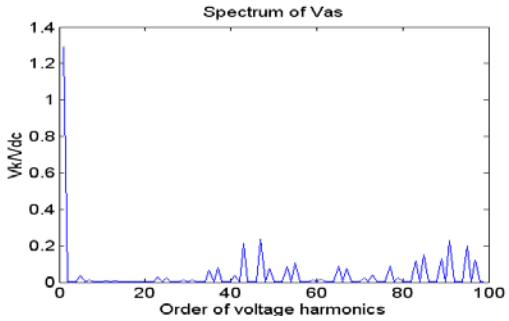

Fig. 18. Spectrum of the phase voltage V_{as} of the system with discontinuous synchronized PWM ($F=50Hz$, $F_s=1.5kHz$, $I_{dc1}=0.6I_{dc2}$, $m_1=0.9$, $m_2=0.54$)

4.5 Spectral assessment of quality of the phase voltage of synchronized dual-inverter system

Total Harmonic Distortion (*THD*) factor of voltage and current is one of the most suitable criteria for analysis of power quality in grid-connected photovoltaic systems. In particular, in accordance with the majority of standards for 50-Hz power systems, total voltage harmonic distortion has to be calculated up to the 40th voltage harmonic [15].

Fig. 19 presents the calculation results of the *THD* factor for the phase voltage V_{as} as a function of modulation index $m=m_1=m_2$, of the dual-inverter system on the base of neutral-clamped inverters with equal dc-currents, controlled by algorithms of continuous (CPWM), "direct-direct" (DDPWM), and discontinuous (DPWM) schemes of synchronized modulation. The *THD* factor ($THD=(1/V_{as_1})\sqrt{\sum_{k=2}^{40} V_{as_k}^2}$) has been calculated until the 40-th low-order (k-th) voltage harmonic. The fundamental frequency of the system is equal to *50Hz*, and the average switching frequency of each modulated inverter are equal correspondingly to *1kHz* and *1.5kHz*.

The presented calculation results show that, for the systems with wide control range (with wide variation of modulation indices of inverters), the discontinuous and

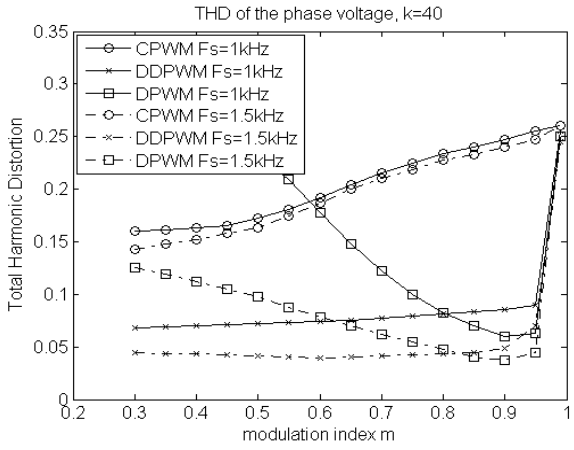

Fig. 19. *THD* factor of the phase voltage V_{as} versus modulation index $m=m_1=m_2$ (CPWM – continuous synchronized PWM, DDPWM – "direct-direct" synchronized PWM, DPWM – discontinuous synchronized PWM)

"direct-direct" schemes of synchronized PWM allow lower *THD* factor of the phase voltage of dual-inverter system in comparison with continuous synchronized pulsewidth modulation.

The calculation results presented in Fig. 19 show also big dependence of the *THD* factor on switching frequency of inverters for the "direct-direct" and discontinuous schemes of synchronized PWM. So, rational choice of switching frequency of cascaded neutral-clamped converters can provide improved effectiveness of operation of dual-inverter-based photovoltaic installations.

5. CONCLUSIONS

Photovoltaic systems on the base of power electronics will play an important role in the future power systems. Behavior of a PV installation is influenced by the chosen topology and modulation strategy of power converters.

Novel topology of grid-connected photovoltaic system is based on two insulated strings of PV panels, each one feeding the dc bus of three-phase inverter. Two inverters are connected to the grid by a three-phase transformer having open-end windings on inverter side.

Novel method of synchronized space-vector modulation, disseminated for control of PV system on the base of two neutral-point-clamped converters, supplied by two photovoltaic dc-sources, allows both continuous phase voltage synchronization (including regimes with fluctuation of the grid fundamental frequency) and system regulation by the corresponding control of modulation indices of the two inverters. The spectra of the phase voltage of the system do not contain even harmonics and sub-harmonics for any operation conditions.

Specialized control strategy, based on the use of only seven voltage vector of each neutral-clamped inverter, provides full elimination of alternating common-mode voltages both in each inverter and in the load.

For PV systems with equal voltages and currents of two dc-sources the discontinuous the "direct-direct" schemes of synchronized PWM provide better spectral composition of the phase voltage in comparison with continuous synchronized modulation.

REFERENCES

[1] A.M. Barnett, *Solar Electric Power for a Better Tomorrow*, Proceedings of the IEEE Photovoltaic Specialists Conference PSC'96, 1996, pp. 1–8.

[2] M. Calais, J. Myrzik, T. Spooner, V.G. Agelidis, *Inverters for single-phase grid connected photovoltaic systems - an overview*, Proceedings of the IEEE Power Electronics Specialists Conference PESC'02, 2002, pp. 1995-2000.

[3] V. Salas, E. Olias, *Overview of the state of technique for PV inverters used in low voltage grid-connected PV systems: Inverters below 10 kW*, Renewable and Sustainable Energy Reviews, 2009, pp. 1-10.

[4] F. Blaabjerg, F. Iov, R. Teodorescu, Zhe Chen, *Power Electronics in renewable energy systems*, Proceedings of the EPE - Power Electronics and Motion Control Conference EPE-PEMC'2006, 2006, pp. 1-17.

[5] F. Blaabjerg, F. Iov, T. Kerekes, R. Teodorescu, *Trends in power electronics and control of renewable energy systems*, Proceedings of the EPE - Power Electronics and Motion Control Conference EPE-PEMC'2010, 2010, pp. K1-K19.

[6] IEA-International Energy Agency, *Trends in photovoltaic applications: survey report of selected IEA countries between 1992 and 2007*, Report IEA-PVPS T1-17, 2008, 17 p.

[7] G. Grandi, D. Ostojic, C. Rossi, A. Lega, *Control strategy for a multilevel inverter in grid-connected photovoltaic applications*, CD-ROM Proceedings of the IEEE Aegean Conference on Electric Machines, Power Electronics and Electromotion, 2007, 6 p.

[8] G. Grandi, C. Rossi, D. Ostojic, D. Casadei, *A new multilevel conversion structure for grid-connected PV applications*, IEEE Transactions on Industrial Electronics, vol. 56, no. 11, 2009, pp. 4416-4426.

[9] V. Oleschuk, G. Grandi, F. Dragonas, *Cascaded neutral-clamped inverters with flexible synchronized PWM for photovoltaic installations*, Proceedings of the IEEE Int'l Symposium on Industrial Electronics ISIE'2011, 2011, pp. 989-993.

[10] K.R.M.N. Ratnayake, Y. Murai, *A novel PWM scheme to eliminate common-mode voltage in three-level voltage source inverter*, Proceedings of the IEEE Power Electronics Specialists Conference PESC'98, 1998, pp. 269-274.

[11] H. Zhang, A. von Jouanne, S. Dai, A.K. Wallace, F. Wang, *Multi-level inverter modulation schemes to eliminate common-mode voltage*, *IEEE Transactions on Industry Application*, vol. 36, no. 6, 2000, pp. 1645-1653.

[12] V. Oleschuk, F. Blaabjerg, *Three-level inverters with common-mode voltage cancellation based on synchronous pulsewidth modulation*, Proceedings of the IEEE Power Electronics Specialists Conference PESC'02, 2002, pp. 863-868.

[13] V. Oleschuk, F. Profumo, A. Tenconi, R. Bojoi, A.M. Stankovic, *Cascaded three-level inverters with synchronized space-vector modulation*, Proceedings of the IEEE Industrial Application Society Conference IAS'2006, 2006, pp. 595-602.

[14] V. Oleschuk, G. Griva, *.Simulation of processes in synchronized cascaded inverters for photovoltaic application*, International Review of Electrical Engineering, vol. 4, no. 5(A), 2009, pp. 928-936.

[15] M. Aiello, A. Cataliotti, S. Favuzza, G. Graditi, *Theoretical and experimental comparison of Total Harmonic Distortion factors for the evaluation of harmonic and interharmonic pollution of grid-connected photovoltaic systems*, IEEE Transactions on Power Delivery, vol. 21, no. 3, 2006, pp. 1390-1397.